DOI: 10.15276/aait.04.2020.2
UDC 004.942:681.51:621.355

IMPROVED STRUCTURE OF PASSIVITY-BASED CONTROL OF BATTERY-SUPERCAPACITOR HUBRID ENERGY STORAGE SYSTEM

Igor Z. Shchur[1)]
ORCID: 0000-0001-7346-1463, ihor.z.shchur@lpnu.ua
Yuriy O. Biletskyi[1)]
ORCID: 0000-0001-6988-0825, yurii.o.biletskyi@lpnu.ua
[1)] National University "Lviv Polytechnic", 12, Bandera St., Lviv, 79013, Ukraine

ABSTRACT

Energy storage systems are a topical modern area of research due to the rapid development of renewable energy and electric vehicle construction. Due to the current lack of a source or accumulator of electricity with high specific energy and power, it is being replaced by hybrid electricity storage systems, which consist of separate, complementary sources. Among them, the combination of electrochemical battery – supercapacitor bank is the most common. The paper considers its active configuration, in which both sources are connected to the output network through bidirectional pulse DC-DC converters. The studied hybrid battery-supercapacitor system is a nonlinear dynamic system with multiple inputs, multiple outputs, and two control channels, the operation of which is described by five differential equations. To solve the problem of synthesis of a stable and efficient control system for such an object, the energy approach, namely energy-shaping control has been used. To do this, the studied system is mathematically described as Port-Controlled Hamiltonian system, and two descriptions are compared with different options for choosing the basic vector of the system state. The structural synthesis of the passive control system was performed by the Interconnection and Damping Assignment method. Based on the energy management strategy developed for the system under study, all possible options for introducing interconnections and damping into the passive control system were explored using a computer program developed in the MathCad environment. The effectiveness of the obtained structures of control influence formers on the investigated dynamic system was studied by computer simulation in the Matlab/Simulink environment. According to the results of the research, the variant of control influence former with the best combination of introduced interconnections and damping is formed according to the principle of superposition. To stabilize the voltage values of the output network and the supercapacitor unit set by the control strategy, a proportional-integrated voltage regulator is additionally used, and a sliding regulator between two passive control structures is exploited to limit the allowable battery current. The results of the computer simulation showed the full implementation of the tasks of the energy management strategy, including a smooth increase and limitation of the battery current.

Keywords: hybrid energy storage system; battery-supercapacitor system; passivity-based control; Port-Controlled Hamiltonian system; Interconnection and Damping Assignment

For citation: **Shchur I. Z., Biletskyi Y. O. Improved Structure of Passivity-Based Control of Battery-Supercapacitor Hybrid Energy Storage System.** ***Applied Aspects of Information Technology.*** **2020; Vol.3 No.4: 232–245.**
DOI: 10.15276/aait.04.2020.2

INTRODUCTION

Energy Storage Systems (ESS) has become a new trend in modern energetics. This is due to the global problem of energy saving. However, the greatest need for the accumulation and storage of electricity has arisen due to the rapid transition from the use of fossil organic energy sources to renewable sources, primarily wind and solar. In the large power industry, the instability of electricity generation by wind and solar installations and stations raises the problem of stability of power grids, which can be solved by the parallel use of high-capacity ESS. In low-power renewable energetics, ESS is an integral part of stand-alone power generation installations. However, most requirements, often contradictory, apply to ESS in autonomous vehicles, in particular in electric vehicles, the mass production of which has already become irreversible [1]. These are high absolute and specific (per unit of mass and volume) energy and power, duration of work (a large number of charge-discharge cycles), non-critical to temperature conditions, as well as low cost. As the combination of these requirements is not provided by any of the known energy sources or accumulators, hybrid ESS hybrid energy storage system (HESS) are often used, usually composed of two sources that complement each other [2]. For example: two different types of batteries (B), B and supercapacitors (SC), fuel cells and SCs, B and ultra-high speed flywheel.

1. LITERATURE OVERVIEW

Among HESS, the B-SC system is one of the most successful and efficient [3-6]. In this system, the B acts as a source of energy, and the SC bank, composed of a number of SCs – as a source of power, because the specific energy of the B is about an order of magnitude higher than that of the SC, and the specific power of the SC is also about an order of magnitude higher than in B. At the same

time, the number of charge-discharge cycles of the SC is approximately two orders of magnitude greater than that of the best batteries, and reaches one million. Therefore, in HESS, the SC bank should take on fast-changing and powerful processes of energy exchange with the load, while the B load should be long and smoothly variable and, if possible, low. This will significantly increase the lifetime of B [7]. Since, unlike B, chemical reactions do not occur in the work of the SC, the latter is not critical to the temperature conditions of operation, keeping their properties practically unchanged under real environmental conditions.

The electrical characteristics of the B and SC bank are also different. The B voltage doesn't vary much depending on the state of charge, while in the SC bank, as in a conventional capacitor, the relationship between its energy w_{sc} and voltage v_{sc} is described by a known expression

$$w_{sc} = \frac{1}{2} C_{sc} v_{sc}^2 \ , \qquad (1)$$

where C_{sc} is the electrical capacity of the SC bank.

Based on (1), in practice, it's tried to ensure such modes of operation of the SC bank; so that it's operating voltage changes no more than twice compared to the maximum. In this case, 75 % of its maximum energy will be available [2].

Due to these different electrical properties of the B and SC bank, different configurations of systems using controlled DC-DC converters as electronic DC transformers are used to combine them in HESS. Among the most popular are the already classic semi-active and fully active configurations (Fig. 1) [8-9]. All of them have advantages and disadvantages. In the most common SC/B configuration (Fig. 1a), due to the B, the voltage of the DC-bus changes not much during operation, but the DC-DC converter must withstand high currents of the SC bank, which increases its cost. In the semi-active configuration of B/SC (Fig. 1b), the DC-DC converter of lower power is used, but the voltage of the DC-bus can vary widely. In a fully active configuration (Fig. 1c), both the B and the SC bank may have a lower voltage compared to the DC-bus voltage, which simplifies the entire system, but two DC-DC converters are required, which increases the cost of HESS. However, the number of degrees of freedom doubles, which allows the use of more advanced control systems.

In addition to the described classical configurations of B-SC HESS, there are others developed recently [9-10]. Among them a separate group worth to mention, called by us the switch structure, in which the B or SC bank can be directly connected to the DC-bus using electronic switches, and exchange energy through a low-power bidirectional DC-DC converter [11]. Switching the structure in such HESS provides different modes of operation in accordance with the branched algorithm of the Energy Management System (EMS). Another interesting group is the cascade structures of HESS, which consist of the described classical, often semi-active configurations, and have a large number of degrees of freedom [12]. This allows HESS to be given additional functions, such as controlling the electric drive powered by this system.

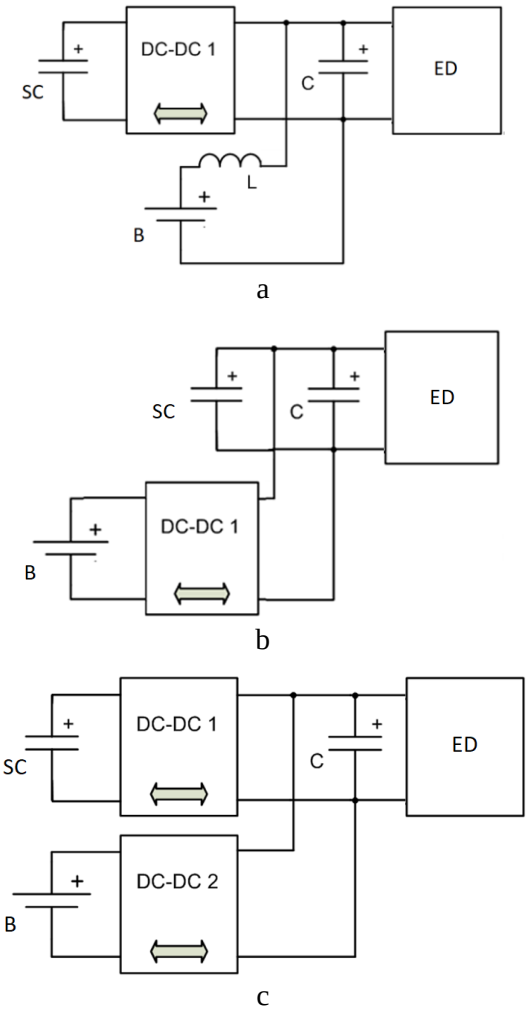

Fig. 1. **Semi-active SC/B (a), semi-active B/SC (b), and fully active (c) HESS configurations**
***Source*: compiled by the author**

In each configuration of B-SC HESS, according to its degrees of freedom, by means of EMS, the necessary control strategy which can include various functions is realized. For example: maintaining a constant voltage of the DC-bus, load distribution between two power supplies, the formation of the dynamics of changes in this load, maintaining a given voltage of the SC bank, etc. [2; 13-15]. Given the diversity of these tasks, as well as the fact that

DC-DC converters are nonlinear dynamic links, the synthesis of HESS control systems is not an easy task. Therefore, the latest modern methods of nonlinear control are used for this: Sliding-Mode Control [16-17], Model Predictive Control [18], Fraction Order Control [19], Fuzzy Logic Control [20], the use of Voltaire series theory and neural networks [21], Flatness Control [22], Passivity-Based Control (PBC) [23]. Among them, PBC and its structural synthesis according to the Interconnection and Damping Assignment (IDA) procedure have a clear understanding of energy patterns during the formation of control effects, as well as ease of asymptotic stability of synthesized systems [24]. According to the IDA-PBC method, many control systems for nonlinear objects have been successfully synthesized, including EMS for control of HESS of a different structure in electric vehicles: fuel cells–SC [25], fuel cells–B [26], B-SC [27].

In our work, we have successfully applied PBC to wind power facilities, as well as to B-SC HESS, which are a multiply input multiply output (MIMO) [23; 28-31]. In particular, in [23], reasonably simple control structures were synthesized for semi-active and fully active configurations of B-SC HESS; in [29], the maximum B current was limited at a given level by sliding switching between two synthesized passive control systems – semi-active and fully active configurations; and in [30], PBC was successfully applied to the cascade structure of B-SC HESS. The acquired experience of passive control allowed us to develop a method of synthesis of all possible control influences that ensure the stability of the system. To do this, in the MathCad computing environment it is necessary to develop an appropriate program that, by symbolic solving a system of nonlinear equations with predetermined interconnections between system elements and damping effects, quickly gives expressions for control effects, if such ensure the stability of the system. The developed methodology allows reviewing the already obtained results of PBC of B-SC HESS in the direction of improving the control strategy of this object.

The purpose of this work is to improve the structure of the PBC system of the fully active configuration of B-SC HESS for better, compared to existing systems, to meet the requirements of energy management strategies. In particular, these are elimination the static error of regulating the set voltage values of the output DC-bus and the SC bank, as well as providing a long time of increase and decrease of the battery current and absence of initial jumps of this current, which will significantly increase the battery lifetime.

To achieve this goal it is necessary to solve the following tasks:

• to develop a method for determining the structures of control influences for the PBC system with a fully active configuration B-SC HESS;

• obtain all possible structures of control influences and select options suitable for practical implementation;

• to investigate the effectiveness of individual elements included in the obtained structures of control influences, and to determine their effective combinations;

• to develop a method of parameters sequential adjustment of control influences elements in effective combinations;

• to confirm the effectiveness of the obtained solutions by computer simulation of a specific B-SC HESS.

2. MATHEMATICAL MODELING OF B-SC HESS AS A PORT-CONTROLLED HAMILTONIAN SYSTEM

2.1. Mathematical description of B-SC HESS of the active configuration

Fig. 2 shows a schematic diagram of the power part of the B-SC HESS of active configuration [5]. This system uses the bidirectional DC-DC converters to connect the B (DC/DC 1) and the SC bank (DC/DC 2) to a DC-bus with the voltage v_{bus}. This allows you to use B and SC bank with the voltages of v_b and v_{sc}, respectively that are lower than v_{bus}. The load in the system is simulated by the back EMF E_l with the internal resistance R_l and inductance L_l.

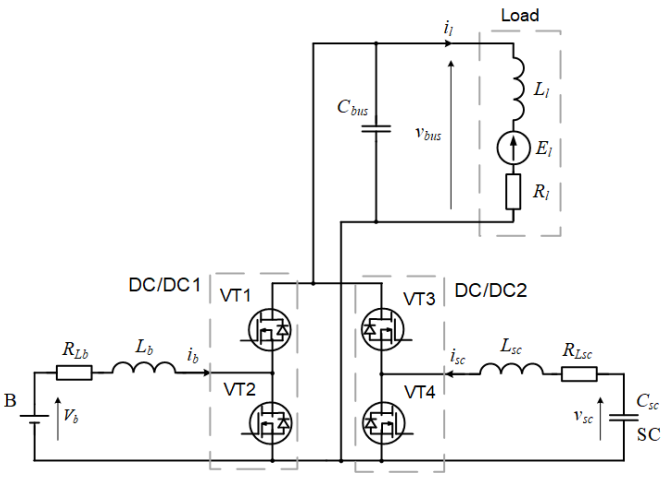

Fig. 2. **Structure of B-SC HESS**
***Source*: compiled by the author**

Given the high frequency of PWM voltage, as well as the continuity of currents in the inductors L_b and L_{sc}, the DC-DC converters can be considered as

ISSN 2617-4316 (Print)
ISSN 2663-7723 (Online)

electronic DC voltage transformers. In this case, instead of the voltage transformation coefficient from the lower side to the higher, the voltage transfer coefficient of the step-up DC-DC converter can be used in the form $(1-\mu)^{-1}$, where μ is the duty cycle of the pulse converter [23]. With this in mind, as well as neglecting the losses in semiconductor devices of the DC-DC converters, the work of B-SC HESS can be described by differential equations, the number of which corresponds to the number of elements in the system that accumulate energy (inductors and capacitors) [23; 29]:

$$\frac{\mathrm{d}}{\mathrm{d}t} i_b = \frac{1}{L_b}\left[V_b - i_b R_b - (1-\mu_1) v_{bus}\right]; \quad (2)$$

$$\frac{\mathrm{d}}{\mathrm{d}t} v_{bus} = \frac{1}{C_{bus}}\left[I_g + (1-\mu_1) i_b + (1-\mu_2) i_{sc} - i_l\right]; \quad (3)$$

$$\frac{\mathrm{d}}{\mathrm{d}t} i_{sc} = \frac{1}{L_{sc}}\left[v_{sc} - i_{sc} R_{Lsc} - (1-\mu_2) v_{bus}\right]; \quad (4)$$

$$\frac{\mathrm{d}}{\mathrm{d}t} v_{sc} = -\frac{1}{C_{sc}} i_{sc}; \quad (5)$$

$$\frac{\mathrm{d}}{\mathrm{d}t} i_l = \frac{1}{L_l}\left(v_{bus} - E_l - R_l i_l\right), \quad (6)$$

where μ_1 and μ_2 are the coefficients of the duty cycle of the DC-DC converters connected to the B and the SC bank, respectively (they form the control vector $\boldsymbol{\mu} = [\mu_1\ \mu_2]$) and i_l is the load current consumed from the DC-bus.

2.2. PCH representation of B-SC HESS

In order to construct the PBC system of B-SC HESS, we present the latter, described by equations (2)-(6), in the form of the port-controlled Hamiltonian (PCH) system [24]:

$$\dot{\mathbf{x}}(t) = \left[\mathbf{J}(\mathbf{x}) - \mathbf{R}(\mathbf{x})\right]\nabla H(\mathbf{x}) + \mathbf{G}(\mathbf{x})\,\mathbf{u}(t), \quad (7)$$

where $\mathbf{x}(t) \in \mathbb{R}^n$ is the system state vector, $\mathbf{J}(\mathbf{x}) \in \mathbb{R}^{n\times n}$ is the skew-symmetric matrix of system interactions, $\mathbf{R}(\mathbf{x}) \in \mathbb{R}^{n\times n}$ is the symmetric positive damping (loss) matrix, $H(\mathbf{x})$ is the energy function of the system (Hamiltonian), $\mathbf{D} \in \mathbb{R}^{n\times n}$ is the diagonal matrix of the system inertias, $\mathbf{G}(\mathbf{x}) \in \mathbb{R}^n$ is the port matrix (inputs/outputs), and $\mathbf{u}(t) \in \mathbb{R}^n$ is the vector of input energy variables in the system.

The first and main step at this stage is to select the state variables that make up the vector $\mathbf{x}$. Here are used two options. We will consider them in turn and compare the results.

According to the first, as state variables, it is possible to select measurable physical variables that determine the amount of energy accumulated in the reactive elements of the system – currents for inductors and voltages for capacitors. In this case, after analyzing the system, a matrix of our AB-SC HESS in the Hamiltonian representation (7) will take the following form:

$$\mathbf{x} = \left[i_b \quad v_{bus} \quad i_{sc} \quad v_{sc} \quad i_l\right]^{\mathrm{T}}; \quad (8)$$

$$\mathbf{u} = \left[V_b \quad 0 \quad 0 \quad 0 \quad -E_l\right]^{\mathrm{T}}; \quad (9)$$

$$\mathbf{D} = \mathrm{diag}\left[L_b \quad C_{bus} \quad L_{sc} \quad C_{sc} \quad L_l\right]. \quad (10)$$

As a result, the total energy function of the system is determined by a quadratic expression

$$H(\mathbf{x}) = \frac{1}{2}\mathbf{x}^{\mathrm{T}}\mathbf{D}\,\mathbf{x} = \frac{1}{2}\left(L_b i_b^{\,2} + C_{bus} v_{bus}^{\,2} + L_{sc} i_{sc}^{\,2} + C_{sc} v_{sc}^{\,2} + L_l i_l^{\,2}\right), \quad (11)$$

and the vector of its partial derivatives consists of energy pulses of the system:

$$\nabla H(\mathbf{x}) = \frac{\partial H(\mathbf{x})}{\partial \mathbf{x}} = \mathbf{D}\mathbf{x} = \left[L_b i_b \quad C_{bus} v_{bus} \quad L_{sc} i_{sc} \quad C_{sc} v_{sc} \quad L_l i_l\right]^{\mathrm{T}}. \quad (12)$$

Based on (7)-(12), we can form the following matrices of the system in the form

$$\mathbf{J}(\boldsymbol{\mu}) = \begin{bmatrix} 0 & -\frac{1-\mu_1}{L_b C_{bus}} & 0 & 0 & 0 \\ \frac{1-\mu_1}{L_b C_{bus}} & 0 & \frac{1-\mu_2}{L_{sc} C_{bus}} & 0 & -\frac{1}{L_l C_{bus}} \\ 0 & -\frac{1-\mu_2}{L_{sc} C_{bus}} & 0 & \frac{1}{L_{sc} C_{sc}} & 0 \\ 0 & 0 & -\frac{1}{L_{sc} C_{sc}} & 0 & 0 \\ 0 & \frac{1}{L_l C_{bus}} & 0 & 0 & 0 \end{bmatrix}; \quad (13)$$

$$\mathbf{R} = \mathrm{diag}\left[R_{Lb}/L_b^2 \quad 0 \quad R_{Lsc}/L_{sc}^2 \quad 0 \quad R_l/L_l^2\right]; \quad (14)$$

$$\mathbf{G} = \mathrm{diag}\left[L_b^{-1} \quad C_{bus}^{-1} \quad 0 \quad 0 \quad L_l^{-1}\right]. \quad (15)$$

According to another approach, state variables should be chosen as energy pulses of the system, such as $i\,L$ and $v\,C$ [31].

In this case, after analyzing the matrix system of our HESS in the Hamiltonian representation will take the following form:

$$\mathbf{x} = \left[i_b L_b \quad v_{bus} C_{bus} \quad i_{sc} L_{sc} \quad v_{sc} C_{sc} \quad i_l L_l\right]^{\mathrm{T}}; \quad (16)$$

$$\mathbf{u} = \left[V_b \quad 0 \quad 0 \quad 0 \quad -E_l\right]^{\mathrm{T}}; \quad (17)$$

$$\mathbf{D} = \mathrm{diag}\left[L_b \quad C_{bus} \quad L_{sc} \quad C_{sc} \quad L_l\right]. \quad (18)$$

As a result, the function of the total energy of the system, which is calculated by a slightly different expression, leads to the same result (11), and the elements of the vector of its partial derivatives are the main variables of the system:

$$H(\mathbf{x}) = \frac{1}{2}\mathbf{x}^{\mathrm{T}}\mathbf{D}^{-1}\mathbf{x} = \frac{1}{2}\left(L_b\, i_b{}^2 + C_{bus}\, v_{bus}{}^2 + L_{sc}\, i_{sc}{}^2 + C_{sc}\, v_{sc}{}^2 + L_l\, i_l{}^2\right); \quad (19)$$

$$\nabla H(\mathbf{x}) = \frac{\partial H(\mathbf{x})}{\partial \mathbf{x}} = \mathbf{D}^{-1}\mathbf{x} = \begin{bmatrix} i_b & v_{bus} & i_{sc} & v_{sc} & i_l \end{bmatrix}^{\mathrm{T}}. \quad (20)$$

The matrices of interconnections, damping and ports will also look different:

$$\mathbf{J}(\boldsymbol{\mu}) = \begin{bmatrix} 0 & \mu_1 & 0 & 0 & 0 \\ -\mu_1 & 0 & -\mu_2 & 0 & -1 \\ 0 & \mu_2 & 0 & 1 & 0 \\ 0 & 0 & -1 & 0 & 0 \\ 0 & 1 & 0 & 0 & 0 \end{bmatrix}; \quad (21)$$

$$\mathbf{R} = \mathrm{diag}\begin{bmatrix} R_{Lb} & 0 & R_{Lsc} & 0 & R_l \end{bmatrix}; \quad (22)$$

$$\mathbf{G} = \mathrm{diag}\begin{bmatrix} 1 & 1 & 0 & 0 & 1 \end{bmatrix}. \quad (23)$$

In order to further compare approaches to the selection of state variables, we will synthesize PBC systems based on the matrices obtained for both cases.

3. SYNTHESIS OF THE PASSIVITY-BASED CONTROL SYSTEM

3.1. Method IDA-PBC

The main idea of passive (energy-shaping) control, in particular IDA-PBC, is the purposeful formation of the energy function of the system and, thus, the impact on the transient and steady-state processes in it [26; 31]. In a closed loop system, the desired energy function H_d is formed such that at its minimum the system is at the desired equilibrium point $\bar{\mathbf{x}}$. The synthesis of the PBC system is to find such additional interconnections and damping that will form the necessary H_d:

$$H_d(\tilde{\mathbf{x}}) = \frac{1}{2}\tilde{\mathbf{x}}^{\mathrm{T}}\mathbf{D}\,\tilde{\mathbf{x}}, \quad (24)$$

where $\tilde{\mathbf{x}} = \mathbf{x} - \bar{\mathbf{x}}$ it is a new state vector defined as the difference between the state vector **x** and the desired vector $\bar{\mathbf{x}}$, what is the control task.

The structure of a closed PBC system, which is a priori asymptotically stable, is described by the following equation [24-32]:

$$\dot{\tilde{\mathbf{x}}}(t) = \left[\mathbf{J}_d(\tilde{\mathbf{x}}) - \mathbf{R}_d(\tilde{\mathbf{x}})\right]\nabla H_d(\tilde{\mathbf{x}}), \quad (25)$$

where $\mathbf{J}_d$ and $\mathbf{R}_d$ are new matrices of interconnections and damping of the desired closed loop system.

The mentioned matrices of interconnections and damping of the desired closed system consist of interconnections and damping of the controlled system and the energy-shaping passive-based control system: $\mathbf{J}_d = \mathbf{J} + \mathbf{J}_a$, $\mathbf{R}_d = \mathbf{R} + \mathbf{R}_a$.

Thus, equating the right-hand sides of equations (6) and (22) we obtain the basic equation for the synthesis of the energy-shaping PBC system [23; 25]:

$$\left(\mathbf{J}_d - \mathbf{R}_d\right)\nabla H_d(\tilde{\mathbf{x}}) = \left[\mathbf{J} - \mathbf{R}\right]\nabla H(\mathbf{x}) + \mathbf{G}(\mathbf{x})\mathbf{u}(t). \quad (26)$$

In order to speed up the synthesis procedure, in the mathematical package MathCad, we have developed a program that allows you to specify the matrices of the controlled object **x**, **u**, **D**, **J**, **R**, **G**, as well as specify the structure of the matrices of the control system $\mathbf{J_a}$ and $\mathbf{R_a}$, and get symbolic solutions of equations (26), in particular the equations of control influence former (CIF), which perform the role of regulators in the PBC system. For this system, these will be expressions for the elements of the matrix **μ**. If it is necessary to take into account the features of the system or the desired control laws, it is possible to set the values/expressions of state variables at the equilibrium point. The program also makes it possible to build regulators with the formation of indirect control effects [32].

3.2. Energy management strategy

In order to form the desired equilibrium point and features of this B-SC HESS, it is advisable to form its EMS tasks:

– PBC system must maintain the DC-bus voltage setpoint V_{bus}^*;

– to ensure accidental producing and absorption of energy with significant changes in load, the control system must maintain the specified voltage value of the SC bank V_{sc}^*;

– the B should provide energy exchange with the load (during a long load) to a given current $I_{b.\max}^*$, but the current change should be slow (which will increase the lifetime of the B), relaying the rapid transients of the load change on the SC bank;

– in the case of increase of the load power and achievement by the battery current the maximum of its value $\pm I_{b.\max}^*$, during the discharge/charge, it is necessary to keep this value at the set level, and the rest of loading power should be fulfilled by the SC block; after reducing the power on the load, the system must leave the limit.

Thus, in accordance with the generated EMS, you can set the following values of state variables at the desired equilibrium point:

$$\bar{\mathbf{x}} = \begin{bmatrix} \left(\dfrac{V_{bus}^* - E_l}{R_l} \cdot \dfrac{V_{bus}^*}{v_b}\right) & V_{bus}^* & 0 & V_{sc}^* & \dfrac{V_{bus}^* - E_l}{R_l} \end{bmatrix}. \quad (27)$$

ISSN 2617-4316 (Print)
ISSN 2663-7723 (Online)

3.3. Synthesis of CIF structures

To synthesize the control system, it is necessary to specify the desired elements in the structure of CIF.

In the general case, the matrices with CIF elements, which determine its structure, can have the following form:

$$\mathbf{J}_a(\boldsymbol{\mu}) = \begin{bmatrix} 0 & -j_{12} & -j_{13} & -j_{14} & -j_{15} \\ j_{12} & 0 & -j_{23} & -j_{24} & -j_{25} \\ j_{13} & j_{23} & 0 & -j_{34} & -j_{35} \\ j_{14} & j_{24} & j_{34} & 0 & -j_{45} \\ j_{15} & j_{25} & j_{35} & j_{45} & 0 \end{bmatrix}; \quad (28)$$

$$\mathbf{R}_a = \operatorname{diag}\begin{bmatrix} r_{11} & r_{22} & r_{33} & r_{44} & r_{55} \end{bmatrix} \quad (29)$$

By setting these or other elements of the matrices $\mathbf{J}_a$ and $\mathbf{R}_a$ zero values, you can change the structure of the CIF of PBC system.

For example, we define the structure when only j_{23} and r_{33} are non-zero elements of matrices. Solving in symbolic form the vector-matrix equation (26) with the help of created in MathCad program, we synthesize the next structures of CIF:

– I) when state variables are i or v:

$$\begin{cases} U_1 = 1 - \mu_1 = \dfrac{v_b}{V_{bus}^*} \\ U_2 = 1 - \mu_2 = \dfrac{V_{sc}^* + j_{23} L_{sc} C_{sc} \left(v_{bus} - V_{bus}^* \right) + r_{33}\, i_{sc} L_{sc}^2}{V_{bus}^*} \end{cases}; \quad (30)$$

– II) when state variables are $i\,L$ or $v\,C$

$$\begin{cases} U_1 = 1 - \mu_1 = \dfrac{v_b}{V_{bus}^*} \\ U_2 = 1 - \mu_2 = \dfrac{V_{sc}^* + j_{23} \left(v_{bus} - V_{bus}^* \right) + r_{33}\, i_{sc}}{V_{bus}^*} \end{cases}. \quad (31)$$

It can be seen, as a result of the synthesis of the energy-shaping system of PBC, simple expressions of the CIF were obtained. For different cases of the selection of state variables, similar expressions (30) and (31) are obtained, which differ only in the presence of constant parameters at the coefficients of the CIF elements, which will be taken into account in their parametric substantiation.

For the PBC system of B-SC HESS, all elements of the matrices $\mathbf{J}_a$ and $\mathbf{R}_a$ have studied alternately with the help of the developed program and thestructures of CIF were obtained, which are summarized in Table. 1. According to its structure, Table. 1 corresponds to the upper right corner of the matrix $\mathbf{J}_a$ (30) together with the diagonal elements corresponding to the matrix $\mathbf{R}_a$ (29).

4. STUDY OF THE OBTAINED STRUCTURES OF CIF BY COMPUTER SIMULATION

To study the obtained CIF structures and find the rational parameters of their elements, a computer model of the B-SC HESS was created in the Matlab/Simulink environment (Fig. 3). To build the model, the subsystems of the electrochemical battery **Battery AB**, the SC bank **Supercapacitor SC** and the DC-DC converters **DC-DC 1** and **DC-DC 2**, available in the latest versions of the SimScape library, were used. The parameters of the experimental B-SC HESS were chosen as follows.

– **Battery**: type Lead-Acid, nominal voltage 24 V, rated capacity 100 Ah;

– **Supercapacitor**: type Maxwell BCAP650K04, nominal voltage 2.7 V, rated capacitance 650 F, equivalent DC series resistance 0.8 mΩ, series-connected SCs in the bank 14;

– **DC-DC convertors**: average model/

Other elements in the model had the following parameters: L_b = 1.0 mH, R_b = 0.02 Ω, L_{sc} = 1.0 mH, R_{sc} = 0.02 Ω, L_l = 1.0 mH, R_l = 0.25 Ω, C_{bus} = 4.7 mF. System references: V_{bus}^* = 48 V, V_{sc}^* = 30 V, $I_{b.\max}^*$ = 40 A.

The investigated variants of CIF are placed in the **Control Subsystem**, which generate control signals U_1 and U_2 for the first **DC-DC 1** and the second **DC-DC 2** DC-DC converters, receiving signals from the current and voltage sensors. The **Battery Current Saturation Subsystem** performs the function of limiting the maximum battery current at the level $\pm I_{b.\max}^*$ (Fig. 4). This is achieved by means of two PI current regulators **PI reg1** and **PI reg2**, respectively, for both directions of current, for which the control switching is carried out by the **Switch3**. Switching to current limiting mode is carried out by two switches **Switch1** and **Switch2** in the sliding mode, which is formed for both directions of current by relay regulators **Relay1** and **Relay2**, respectively, for both directions of current. The transition of the system to the battery current limiting mode actually reduces by one the order of the PBC system (from 5 to 4) [29].

Analysis of the obtained CIF structures presented in Table. 1 shows that only a small part of them are effective, i.e. has an additional effect compared to the basic CIF (32). These are CIFs with interconnections j_{12} (33), j_{14} (34), j_{23} (35), j_{34} (36), and damping r_{33} (37). CIFs with other interconnections and dampings are either ineffective, i.e. have a basic structure (32), or do not exist, or their structure is complex and not suitable for practical implementation (requires many coordinate sensors).

Table 1. **The obtained CIF structures for all elements of the matrices J_a and R_a**

	2	3	4	5
1	$U_1 = \frac{v_b}{V_{bus}^*} + j_{12}\frac{\left(v_{bus} - V_{bus}^*\right)}{V_{bus}^*}$, $U_2 = \frac{V_{sc}^*}{V_{bus}^*}$. (33)	Complex implementation	$U_1 = \frac{v_b}{V_{bus}^*} + j_{14}\frac{\left(v_{sc} - V_{sc}^*\right)}{V_{bus}^*}$, $U_2 = \frac{V_{sc}^*}{V_{bus}^*}$. (32)	Does not exist
2	$U_1 = \frac{v_b}{V_{bus}^*}$, (32) $U_2 = \frac{V_{sc}^*}{V_{bus}^*}$.	$U_1 = \frac{v_b}{V_{bus}^*}$, (35) $U_2 = \frac{V_{sc}^*}{V_{bus}^*} + j_{23}\frac{\left(v_{bus} - V_{bus}^*\right)}{V_{bus}^*}$.	$U_1 = \frac{v_b}{V_{bus}^*}$, (32) $U_2 = \frac{V_{sc}^*}{V_{bus}^*}$.	$U_1 = \frac{v_b}{V_{bus}^*}$, (32) $U_2 = \frac{V_{sc}^*}{V_{bus}^*}$.
3		$U_1 = \frac{v_b}{V_{bus}^*}$, (37) $U_2 = \frac{V_{sc}^*}{V_{bus}^*} + \frac{r_{33}\, i_{sc}}{V_{bus}^*}$.	$U_1 = \frac{v_b}{V_{bus}^*}$, (36) $U_2 = \frac{V_{sc}^*}{V_{bus}^*} + j_{34}\frac{\left(v_{sc} - V_{sc}^*\right)}{V_{bus}^*}$.	Complex implementation
4			$U_1 = \frac{v_b}{V_{bus}^*}$, (32) $U_2 = \frac{V_{sc}^*}{V_{bus}^*}$.	$U_1 = \frac{v_b}{V_{bus}^*}$, (32) $U_2 = \frac{V_{sc}^*}{V_{bus}^*}$.
5				$U_1 = \frac{v_b}{V_{bus}^*}$, (32) $U_2 = \frac{V_{sc}^*}{V_{bus}^*}$.

***Source*: compiled by the author**

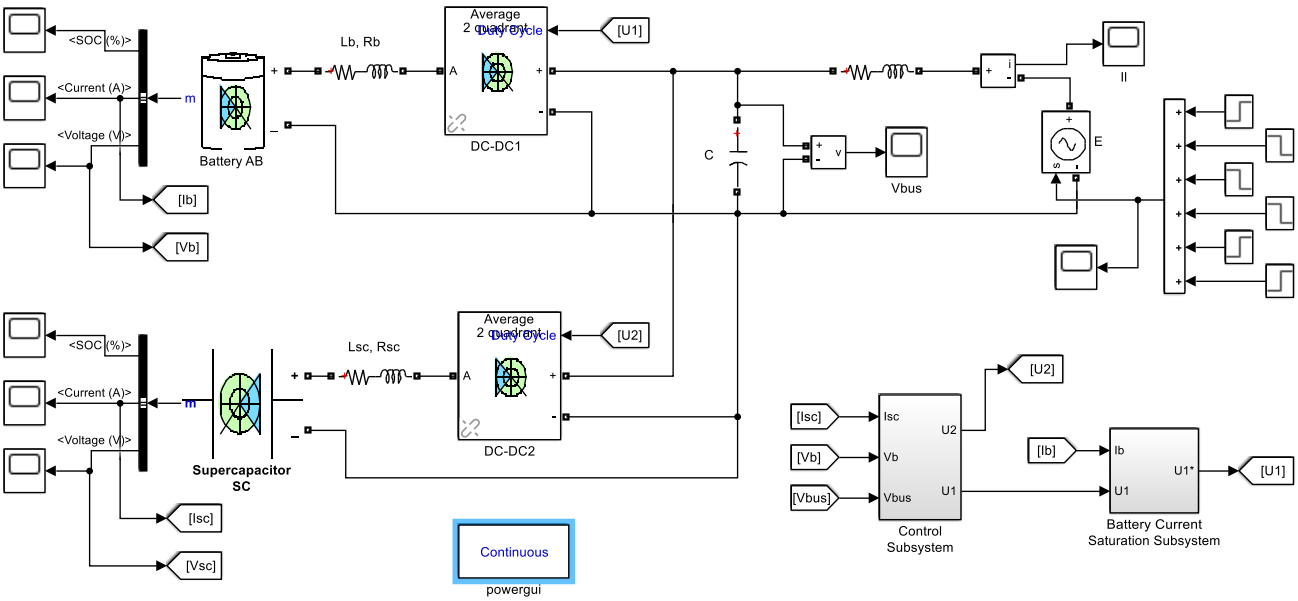

Fig. 3. **Computer model of B-SC HESS**
***Source*: compiled by the author**

ISSN 2617-4316 (Print)
ISSN 2663-7723 (Online)

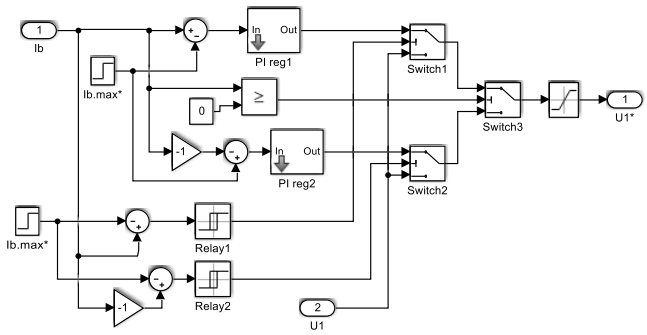

Fig. 4. **Battery Current Saturation Subsystem**
***Source*: compiled by the author**

If we compare them with the structure of the interconnections of the object (13) and (21), the CIF interconnections j_{12}, j_{23} and j_{34} correspond to those already present in the object, i.e. they can adjust their action. And only interconnection j_{14} is new, which is not in the object.

To ensure the formed control strategy, it is necessary to investigate on the created computer model, what action on the B-SC HESS is exerted by separate effective elements of CIF, and then to choose their best combination. Since these elements form an additional effect to the basic CIF (32), the basis for comparison will be the results of the experimental B-SC HESS with the basic CIF, which are presented in Fig. 5 (when the battery current saturation is turned off). As can be seen from the obtained time diagrams, under the influence of the test load (Fig. 5a), which changes rapidly every 10 s, the studied system maintains the voltages of DC-bus and SC bank at specified levels of 48 V and 30 V respectively with large static errors (Fig. 5b and Fig.5d). Rapid changes in the load current (Fig. 3f) are handled by the SC bank (Fig. 5d), while the battery current changes smoothly, but at the beginning of each transient has a jump equal to about half the steady-state (Fig. 5c).

Thus, the basic CIF basically performs all the functions provided by the formed EMS, but there are the above shortcomings in the transient and steady-state modes of operation. In addition, the basic CIF is not able to influence the load distribution between the B and the SC bank in a steady-state, as well as change the dynamics of transients, especially the time of increase or decrease of the battery current, which is an important condition for its saving work. We will try to solve these problems by means of other variants of the received effective CIF structure.

The interconnection j_{12} connects the variables of the battery current and the DC-bus voltage. Fig. 6 presents time diagrams of some variables according to the CIF (33), which is realized by means of the DC-bus voltage feedback, where j_{12} = - 0.35. If we compare the results with those corresponding to the basic CIF, it is seen that the interconnection j_{12} provides some deceleration of transients, reducing the battery current in steady-state, and reduces the initial jump of this current by increasing the initial current jump of the SC bank, which is a positive result. However, this is accompanied by a negative result – an increase in voltage errors of the DC-bus and the SC bank in steady-state.

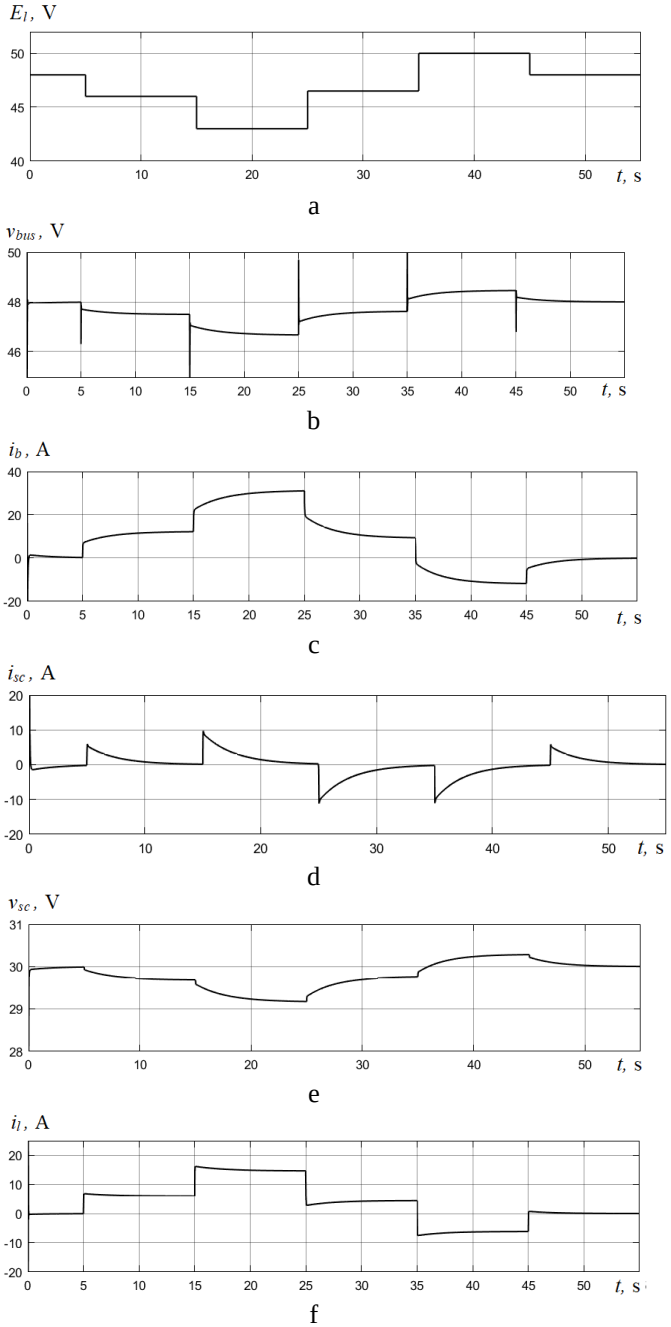

Fig. 5. **Time diagrams of main variables during the operation of the experimental B-SC HESS with the base CIF (32)**
***Source*: compiled by the author**

The interconnection j_{14} connects the variables of the battery current and the SC bank voltage and is realized by SC bank voltage feedback. As shown by

the results of computer simulation for the CIF (34) with j_{14} = - 0.5, the interconnection j_{14} accelerates the transients and increases the relative magnitude of the jump of this battery current at the beginning of the transients. However, it reduces the voltage errors of the DC-bus and the SC bank in steady-state modes. That is, the effect of this interconnection is the opposite of the interconnection j_{12}.

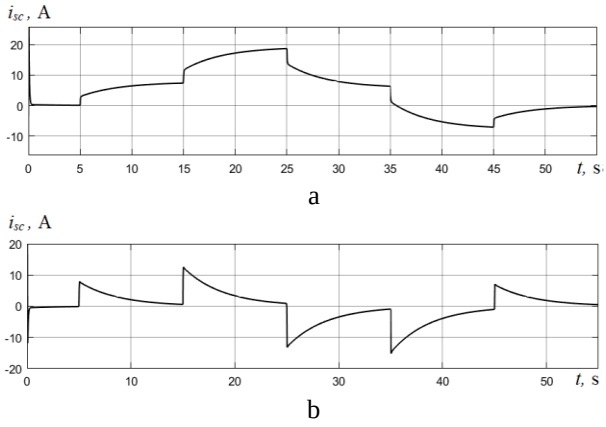

Fig. 6. **Selected time diagrams of main variables during the operation of the experimental B-SC HESS with CIF with interconnection j_{12}**
***Source*: compiled by the author**

The interconnection j_{23} connects the variables of the SC bank current and the DC-bus voltage. Fig.7 shows the time diagrams of some variables according to the CIF (35) with j_{23} = 0.5, which is realized by means of feedback on the DC-bus voltage. If we compare the results with those corresponding to the base CIF, it is seen that the interconnection j_{23} stretches the transient process of the battery current change (switching the load in Fig. 7 is carried out every 20 s), but does not affect its value, as well as the voltage error of the DC-bus. It also does not affect the initial current jumps in the SC bank, but significantly increases the voltage errors of the SC bank in steady-state.

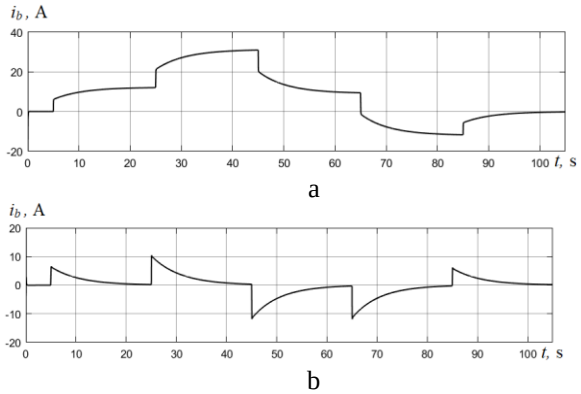

Fig. 7. **Selected time diagrams of main variables during the operation of the experimental B-SC HESS with CIF with interconnection j_{23}**
***Source*: compiled by the author**

The interconnection j_{34} connects the current and voltage variables of the SC bank and is realized by feedback on the SC bank voltage. As shown by the results of computer simulation for the CIF (36) with j_{34} = 0.6, the interconnection j_{34} provides some deceleration of transients, has almost no effect on the battery current in steady-state and transient modes, as well as the DC-bus voltage. However, it provides an increase in the initial current jump in the SC bank, accompanied by an increase in the voltage error of the SC bank in steady-state.

The damping r_{33} connects the current and voltage variables of the SC bank. Fig. 8 presents time diagrams of some variables according to the CIF (37), which is realized by means of feedback on the SC-block current, where r_{33} = - 0.03. If we compare the obtained results with those corresponding to the basic CIF, it is seen that the interconnection j_{34} of this polarity forces the transients in the whole system by increasing the initial current jumps in the SC bank. The voltage errors of the DC-bus and the SC bank in steady-state modes are practically unaffected.

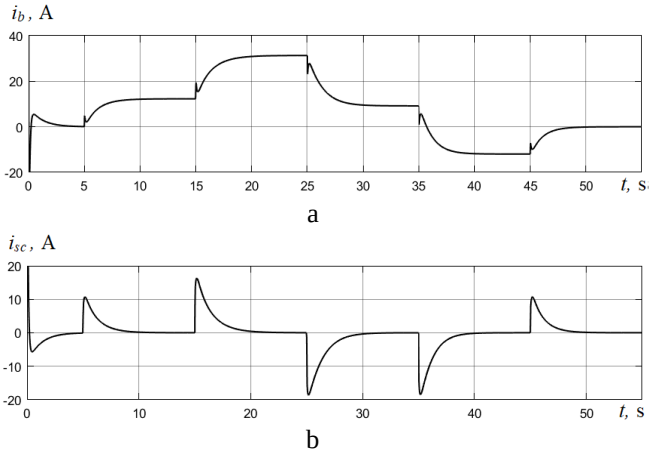

Fig. 8. **Selected time diagrams of main variables during the operation of the experimental B-SC HESS with CIF with damping r_{33}**
***Source*: compiled by the author**

The analysis of results of the carried-out researches of the received CIFs shows that interconnections j_{12}, j_{23}, j_{34} and damping r_{33}, are the most suitable for the tasks of the formed EMS, while the interconnection j_{14} shows a contradictory result – improves one at the expense of the other. Since the main function of the interconnections j_{23} and j_{34} in the control system is to slow down the transients of the current change in the B. To obtain the final CIF we use the superposition of the CIFs with the interconnections j_{12} and j_{23}, which are realized by joint feedback on DC-bus, as well as damping r_{33}:

ISSN 2617-4316 (Print)
ISSN 2663-7723 (Online)

$$\begin{cases} U_1 = \dfrac{v_b}{V^*_{bus}} + j_{12}\dfrac{\left(v_{bus} - V^*_{bus}\right)}{V^*_{bus}} \\ U_2 = \dfrac{V^*_{sc}}{V^*_{bus}} + j_{23}\dfrac{\left(v_{bus} - V^*_{bus}\right)}{V^*_{bus}} + \dfrac{r_{33}\, i_{sc}}{V^*_{bus}} \end{cases}. \quad (38)$$

5. SYNTHESIS OF THE FINAL CIF AND THE SIMULATION RESULTS OF THE STUDIED B-SC HESS

Computer experiments have shown that it is advisable to adjust the CIF parameters in the following sequence.

1. By setting in (40) j_{23} = 0 and r_{33} = 0, choose the value of the interconnection j_{12}, which will provide the desired value of the battery current for a given load current.

2. For the obtained value of j_{12}, choose a value of r_{33} that will remove the initial jumps of the battery current.

3. For the obtained values of j_{12} and r_{33}, choose a value of j_{23} that will provide the required duration of transients, i.e. the smoothness of the increase in the battery current.

For the experimental B-SC HESS, by the described method, the following settings of the CIF (38) were obtained: j_{12} = -0.35, j_{23} = 1.0 and r_{33} = -0.035. The results of the HESS simulation showed that the PBC system provides the required smoothness of the battery current change and its reduced values due to the operation of the SC bank. However, there are significant errors in the set values of the DC-bus voltage and the SC bank voltage. To reduce them, it is advisable to introduce integral components into the control system. Testing of a number of variants of their inclusion showed that it is enough to introduce only one integral component into the feedback channel on the DC-bus voltage in parallel to the interconnection j_{12}, as can be seen from the computer model of the final CIF in Fig. 9.

Experiments have shown that a coefficient of 0.02 is sufficient for the integral component. The results of the simulation of B-SC HESS with the final CIF (38) during the experimental period are shown in Fig. 10. Testing was performed with the same changes in the EMF load (Fig. 10a), but with a much larger step of its change – 60 s, because the synthesized PBC system provides the desired smoothness of the change in the battery current.

In the time interval 84…141 s, the system limits the battery current to a given level of 40 A (Fig. 10c). The current coming from the output of the converter DC-DC1 to the load is limited accordingly. The remaining load current is provided by the SC bank (Fig. 10d), the voltage of which remains at 29 V (Fig. 10e). After the end of the current limitation of the battery voltage, the voltage of the SC bank is gradually restored to a given level of 30 V due to its charging from the B through the DC-bus.

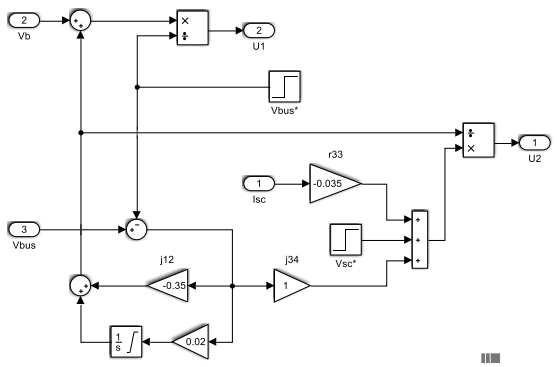

Fig. 9. **Control Subsystem with the final CIF (38)**
***Source*: compiled by the author**

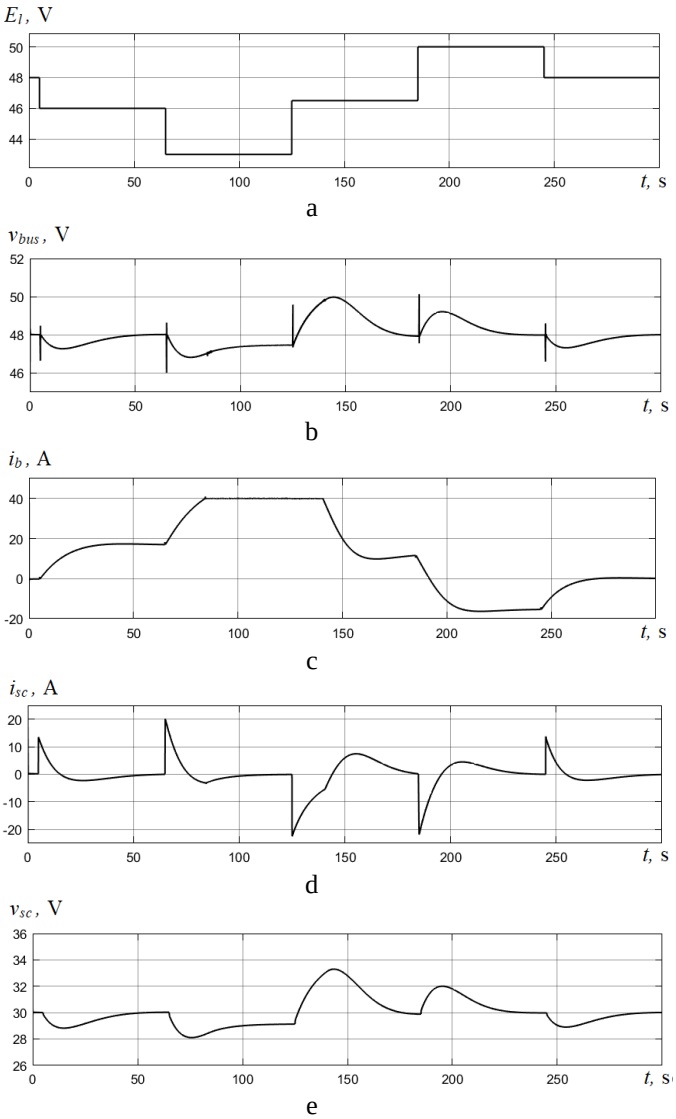

Fig. 10. **Time diagrams of main variables during the operation of the experimental B-SC HESS with the final CIF (38)**
***Source*: compiled by the author**

From the obtained time diagrams it is seen that the PBC system provides all the requirements formed by the EMS, including the required accuracy of maintaining the set values of DC-bus voltage (Fig. 10b) and the voltage of the SC-block (Fig. 10e).

CONCLUSIONS

The developed method of structural synthesis of the PBC system has shown its effectiveness, as it provided a quick solution in the symbolic form of a complex vector-matrix equation and obtaining all possible variants of CIF. The study of the latter by computer simulation made it possible to form based on superposition a variant of the CIF with the best combination of interconnections and damping. In addition, the problem of stabilizing the voltages of the DC-bus and the SC bank and limiting the maximum value of the battery current has also been successfully solved.

The results of computer simulation of the experimental B-SC HESS showed that the proposed approach has significantly improved the performance of the PBC system on the set of tasks that were laid down in the energy management strategy. In particular, such a structure of the CIF was found, which allows to set the required long time of increase and decrease of the battery current and insures absence of initial jumps of this current, which will significantly increase the battery lifetime. Thus for realization of PBC system, it is necessary to apply three coordinate sensors: B voltage, SC bank current, and the DC-bus voltage.

REFERENCES

1. Nazarova, O. S., Osadchyy, V. V. & Brylystyi, V. V. “Computer simulation of electric vehicle acceleration processes with different positions of the mass center”. *Applied Aspects of Information Technology. Publ. Nauka i Tekhnika*. Odessa. Ukraine: 2020; Vol. 3 No. 3: 154–164. DOI: 10.15276/aait.01.2020.4.

2. Hemmati, R. & Saboori, H. “Emergence of hybrid energy storage systems in renewable energy and transport applications – A review”. *Renewable and Sustainable Energy Reviews*. 2016; Vol.65: 11–23. DOI: 10.1016/j.rser.2016.06.029.

3. Cabrane, Z., Ouassaid, M. & Maaroufi M. “Analysis and evaluation of battery-supercapacitor hybrid energy storage system for photovoltaic installation”. *Intern. Journal of Hydrogen Energy*. 2016; Vol. 41: 20897–20907. DOI: 10.1016/j.ijhydene.2016.06.141.

4. Ma, T., Yang, H. & Lu, L. “Development of hybrid battery–supercapacitor energy storage for remote area renewable energy systems”. *Applied Energy*. 2015; Vol. 153: 56–62. DOI: 10.1016/j.apenergy.2014.12.008.

5. Asensio, M., Magallán, G., Amaya, G. & De Angelo, C. “Efficiency and Performance Analysis of Battery-Ultracapacitor based Semi-active Hybrid Energy Systems for Electric Vehicles“. *IEEE Latin America Transactions*. 2018; Vol. 16 No.10: 2581–2590. DOI: 10.1109/TLA.2018.8795138.

6. Khalid, M. “A Review on the Selected Applications of Battery-Supercapacitor Hybrid Energy Storage Systems for Microgrids”. *Publ. Energies.* 2019; Vol. 2 No.23: 1–34. DOI:10.3390/en12234559.

7. Ongaro, F., Saggini, S. & Mattavelli, P. “Li-Ion Battery-Supercapacitor Hybrid Storage System for a Long Lifetime, Photovoltaic-Based Wireless Sensor Network”. *IEEE Trans. Power Electron*. 2012; Vol.27 No.9: 3944–3952. DOI: 10.1109/TPEL.2012.2189022.

8. Peresada, S., Nikonenko, Y., Kovbasa, S., Kuznietsov, A. & Pushnitsyn, D. “Rapid Prototyping Station for Batteries-Supercapacitors Hybrid Energy Storage Systems” *Proc. 2019 IEEE 39th International Conference on Electronics and Nanotechnology (ELNANO)*. Kyiv. Ukraine: 2019. p. 826-831. DOI: 10.1109/ELNANO.2019.8783731.

9. Kouchachvili, L., Yaïci, W. & Entchev, E. “Hybrid battery/supercapacitor energy storage system for the electric vehicles”. *Journal of Power Sources.* 2018; Vol.374: 237–248. DOI: 0.1016/j.jpowsour.2017.11.040.

10. Song, Z., Li, J., Han, X., Xu, L., Lu, L. & Ouyang, M. “Multi-objective optimization of a semi-active battery/supercapacitor energy storage system for electric vehicles”. *Applied Energy*. 2014; Vol.135: 212-224. DOI: 10.1016/j.apenergy.2014.06.087.

11. Shchur, I., Bilyakovskyy, I. & Turkovskyi, V. “Improvement of Switched Structure Semi-Active Battery/Supercapacitor Hybrid Energy Storage System for Electric Vehicles”. *IET Electrical Systems in Transportation* (article in press).

ISSN 2617-4316 (Print)
ISSN 2663-7723 (Online)

12. Shchur, I. & Turkovskyi, V. “Multilevel DC Link Inverter Fed BLDC Motor Drive with Modular Battery/Supercapacitor HESS for Electric Vehicle”. *25th IEEE International Conference on Problems of Automated Electric Drive. Theory and Practice (PAEP’20)*. Kremenchuk. Ukraine: 2020. p. 1-6. DOI: 10.1109/PAEP49887.2020.9240871.

13. Castaings, A., Lhomme, W., Trigui, R. & Bouscayrol, A. “Comparation of energy management strategies of a battery/supercapacitors system for electric vehicle under real-time constraints”. *Applied Energy*. 2016;Vol. 63:190–200. DOI: 10.1016/j.apenergy.2015.11.020.

14. Kollimalla, S. K., Mishra, M. K. & Narasamma, N. L. “Design and analysis of novel control strategy for battery and supercapacitor storage system”. *IEEE Trans. Sustainable Energy*. 2014; Vol.5 No.4: 1137–1144. DOI: 10.1109/TSTE.2014.2336896.

15. Lahyani, A., Sari, A., Lahbib, I. & Venet, P. “Optimal hybridization and amortized cost study of battery/supercapacitors system under pulsed loads”. *Journal of Energy Storage*. 2016; Vol.6: 222–231. DOI: 10.1016/j.est.2016.01.007.

16. Song, Z., Hou, J., Hofman, H., Li, J. & Ouyang, M. “Sliding-mode and Lyapunov function-based control for battery/supercapacitor hybrid energy storage system used in electric vehicles”. *Publ. Energy*. 2017; Vol.122: 601–612. DOI: 10.1016/j.energy.2017.01.098.

17. Wang, B., Xu, J., Xu, D. & Yan. Z. “Implementation of an estimator-based adaptive sliding mode control strategy for a boost converter based battery/supercapacitor hybrid energy storage system in electric vehicles”. *Energy Conversion and Management*. 2017; Vol.151: 562–572. DOI: 10.1016/j.enconman.2017.09.007.

18. Zhang, L., Xia, X. & Barzegar, F. “Control of a battery/supercapacitor hybrid energy storage system for electric vehicles” *Proc. 36th Chinese Control Conference*. Dalian. China: 2017. p. 9560–9565. DOI: 10.23919/ChiCC.2017.8028883.

19. Yang, B., Wang, J., Zhang, X., Wang, J., Shu, H., Li, Sh., He, T., Lan, Ch. & Yu, T. “Applications of battery/supercapacitor hybrid energy storage systems for electric vehicles using perturbation observer based robust control”. *Journal of Power Sources.* 2020; Vol.448. DOI: 10.1016/j.jpowsour.2019.227444.

20. Thounthong, P., Luksanasakul, A., Koseeyaporn, P. & Davat, B. “Intelligent model-based control of a standalone photovoltaic/fuel cell power plant with supercapacitor energy storage”. *IEEE Trans. Sustainable Energy*. 2013; Vol.4 No.1: 240–249. DOI: 10.1109/TSTE.2012.2214794.

21. Ruban, O. D. “Volterra Neural Network Construction in the Nonlinear Dynamic Systems Modeling Problem”. *Applied Aspects of Information Technology*. 2019; Vol. 2 No.1: 24–28. DOI: 10.15276/hait.01.2019.2.

22. Benaouadj, M., Aboubou, A., Ayad, M.Y. & Becherif, M. “Nonlinear flatness control applied to supercapacitor contribution in hybrid power systems using photovoltaic source and batteries”. *Energy Procedia.* 2014; Vol. 50: 333–341. DOI: 10.1016/j.egypro.2014.06.040.

23. Shchur, I. & Biletskyi, Y. “Interconnection and damping assignment passivity based control of semi-active and active battery-supercapacitor hybrid energy storage systems for stand-alone photovoltaic installations”. *Proc. 14th IEEE Int. Conf. on Advanced Trends in Radioelectronics, Telecommunications and Computer Engineering (TCSET-2018)*. Lviv. Ukraine: 2018. p.1–6. DOI: 10.1109/TCSET.2018.8336212.

24. Ortega, R., van der Schaft, A., Mareels, I. & Maschke, B. “Putting energy back in control”. *IEEE Contr. Syst. Mag.* 2001; Vol.21 No.2:18–33. DOI: 10.1109/37.915398.

25. Benmouna, A., Becherif, M., Depature, C., Boulon, L. & Depernet D. “Experimental study of energy management of FC/SC hybrid system using the Passivity Based Control”. *International Journal of Hydrogen Energ.* 2018; Vol.43(25):11583-11592. DOI: https://doi.org/10.1016/j.ijhydene.2018.03.191.

26. Benmouna, A., Becherif, M., Depernet, C. & Ebrahim, M. A. “Novel Energy Management Technique for Hybrid Electric Vehicle via Interconnection and Damping Assignment Passivity Based Control”. *Renewable Energy.* 2018; Vol.119: 116–128. DOI: 10.1016/j.renene.2017.11.051.

27. Wu, T., Cheng, Z., Zhang, J. & He, Z. “A PCH strong tracking control strategy for power coordinated allocation of Li-SC HESS”. *Microelectronics Reliability.* 2018; Vol.88–90: 1261–1267. DOI: 10.1016/j.microrel.2018.06.066.

28. Shchur, I., Rusek, A., & Biletskyi, Y. “Energy-shaping optimal load control of PMSG in a stand-alone wind turbine as a port-controlled Hamiltonian system”. *Przegląd elektrotechniczny (Electrical review)*. 2014; No.5:50–55. DOI: 10.12915/pe.2014.05.10.

29. Shchur, I. & Biletskyi, Y. “Battery current limitation in passivity-based controlled battery/supercapacitor hybrid energy storage system”. *Proc. 38th IEEE Int. Conf. on Electronics and*

Nanotechnology (ELNANO-2018). Kyiv. Ukraine: 2018. p. 504–510. DOI: 10.1109/ELNANO.2018.8477477.

30. Shchur, I., Kulwas, D. & Wielgosz R. "Combination of distributed MPPT and distributed supercapacitor energy storage based on cascaded converter in photovoltaic installation". *Proc. IEEE 3rd Int. Conf. Intelligent Energy and Power Systems (IEPS)*. Kharkiv. Ukraine: 2018. p. 139–144. DOI: 10.1109/IEPS.2018.8559513.

31. Shchur, I. & Biletskyi, Y. "Energy-Shaping Control of Electromechanical Systems with Permanent Magnet Synchronous Motors". Monografy. *Taras Soroka Press*. Lviv. Ukraine: 2018. 172 p. (in Ukrainian).

32. Shchur, I., Biletskyi, Y. & Golovach, I. "Improving of IDA-PBC systems by forming additional regulatory actions on directly uncontrollable system loops". *Proc. 2017 IEEE First Ukraine Conf. on Electrical and Computer Engineering (UKRCON)*. Kyiv. Ukraine: 2017. p. 504–507. DOI: 10.1109/UKRCON.2017.8100291.

Conflicts of Interest: the authors declare no conflict of interest

Received 08.10.2020
Received after revision 12.11.2020
Accepted 20.11. 2020

DOI: 10.15276/aait.04.2020.2
УДК 681.51:621.355

УДОСКОНАЛЕНА СТРУКТУРА ПАСИВНОГО КЕРУВАННЯ ГІБРИДНОЮ АКУМУЛЯТОРНО-СУПЕРКОНДЕНСАТОРНОЮ СИСТЕМОЮ ЗБЕРІГАННЯ ЕНЕРГІЇ

Ігор Зенонович Щур[1)]
ORCID: 0000-0001-7346-1463, ihor.z.shchur@lpnu.ua
Юрій Олегович Білецький[1)]
ORCID: 0000-0001-6988-0825, yurii.o.biletskyi@lpnu.ua
[1)] Національний університет «Львівська політехніка», вул. С. Бандери, 12, Львів, 79013, Україна

АНОТАЦІЯ

Системи зберігання електричної енергії є актуальним сучасним напрямком досліджень, зумовленим стрімким розвитком відновлюваної енергетики та електромобілебудування. Через відсутність на даний час джерела чи нагромаджувача електроенергії з високими питомими показниками енергії та потужності, його замінюють гібридними системами зберігання електричної енергії, які складаються з окремих джерел, що доповнюють одне одного. Серед них комбінація електрохімічна акумуляторна батарея – суперконденсаторний блок є найбільш поширеною. У роботі розглядається її активна конфігурація, у якій обидва джерела підключені до вихідної мережі через двонапрямлені імпульсні перетворювачі постійної напруги. Досліджувана гібридна акумуляторно-суперконденсаторна система є нелінійною динамічною системою з багатьма входами і багатьма виходами та двома каналами керування, робота якої описана п'ятьма диференціальними рівняннями. Для вирішення задачі синтезу стабільної та ефективної системи керування для такого об'єкта у роботі застосовано енергетичний підхід, а саме енергоформуюче керування. Для цього досліджувана система математично описана як гамільтонова система з керованими портами, причому порівняно два описи з різними варіантами вибору базового вектора стану системи. Структурний синтез системи пасивного керування проводився за методом формування взаємозв'язків та введення демпфувань. На основі сформованої для досліджуваної системи стратегії енергетичного менеджменту за допомогою розробленої в середовищі MathCad комп'ютерної програми були досліджені усі можливі варіанти введення енергетичних взаємозв'язків та демпфувань у систему пасивного керування. Дієвість отриманих структур формувачів керуючих впливів на досліджувану динамічну систему вивчалася шляхом комп'ютерного симулювання в середовищі Matlab/Simulink. За результатами дослідження сформовано за принципом суперпозиції варіант формувачів керуючих впливів з найкращою комбінацією введених взаємозв'язків та демпфувань. Для стабілізації заданих стратегією керування значень напруг вихідної мережі та суперконденсаторного блока додатково застосовано пропорційно-інтегральний регулятор напруги, а для обмеження допустимого струму акумуляторної батареї – ковзний регулятор між двома структурами пасивного керування. Результати комп'ютерного симулювання показали повне виконання завдань стратегії енергетичного менеджменту, зокрема плавне наростання та обмеження струму акумуляторної батареї.

Ключові слова: гібридна система зберігання енергії; акумуляторно-суперконденсаторна система; пасивне керування; гамільтонова система з керованими портами; синтез взаємозв'язків і демпфування

ISSN 2617-4316 (Print)
ISSN 2663-7723 (Online)

DOI: 10.15276/aait.04.2020.2
УДК 681.51:621.355

УСОВЕРШЕНСТВОВАННАЯ СТРУКТУРА ПАССИВНОГО УПРАВЛЕНИЯ ГИБРИДНОЙ АККУМУЛЯТОРНО-СУПЕРКОНДЕНСАТОРНОЙ СИСТЕМОЙ ХРАНЕНИЯ ЭНЕРГИИ

Игорь Зенонович Щур[1)]
ORCID: 0000-0001-7346-1463, ihor.z.shchur@lpnu.ua
Юрий Олегович Билецкий[1)]
ORCID: 0000-0001-6988-0825, yurii.o.biletskyi@lpnu.ua
[1)] Національний університет «Львівська політехніка», ул. С. Бандеры, 12, Львов, 79013, Украина

АННОТАЦИЯ

Системы хранения электрической энергии являются актуальным современным направлением исследований, обусловленным стремительным развитием возобновляемой энергетики и электромобилестроения. Из-за отсутствия в настоящее время источника или накопителя электроэнергии с высокими удельными показателями энергии и мощности, его заменяют гибридными системами хранения электрической энергии, состоящими из отдельных источников, дополняющих друг друга. Среди них комбинация электрохимическая аккумуляторная батарея – суперконденсаторный блок является наиболее распространенной. В работе рассматривается ее активная конфигурация, в которой оба источника подключены к выходной сети через двунаправленные импульсные преобразователи постоянного напряжения. Исследуемая гибридная аккумуляторно-суперконденсаторная система является нелинейной динамической системой со многими входами, многими выходами и двумя каналами управления, работа которой описана пятью дифференциальными уравнениями. Для решения задачи синтеза стабильной и эффективной системы управления для такого объекта, в работе применен энергетический подход, а именно енергоформирующее управление. Для этого исследуемая система математически описана как гамильтонова система с управляемыми портами, причем подвергнуты сравнению два описания с различными вариантами выбора базового вектора состояния системы. Структурный синтез системы пассивного управления проводился по методу формирования взаимосвязей и введения демпфирований. На основе сформированной для исследуемой системы стратегии энергетического менеджмента с помощью разработанной в среде MathCad компьютерной программы были исследованы все возможные варианты введения энергетических взаимосвязей и демпфирований в систему пассивного управления. Действенность полученных структур формирователей управляющих воздействий на исследуемую динамическую систему изучалась путем компьютерного симулирования в среде Matlab/Simulink. В результате исследования сформирован по принципу суперпозиции вариант формирователей управляющих воздействий с лучшей комбинацией введенных взаимосвязей и демпфирований. Для стабилизации заданных стратегией управления значений напряжений выходной сети и суперконденсаторного блока дополнительно применен пропорционально-интегральный регулятор напряжения, а для ограничения допустимого тока аккумуляторной батареи – скользящий регулятор между двумя структурами пассивного управления. Результаты компьютерного симулирования показали полное выполнение задач стратегии энергетического менеджмента, в частности плавное нарастание и ограничения тока аккумуляторной батареи.

Ключевые слова: гибридная система хранения энергии; аккумуляторно-суперконденсаторная система; пассивное управление; гамильтонова система с управляемыми портами; синтез взаимосвязей и демпфирования.

ABOUT THE AUTHORS

Ihor Zenonovich Shchur – Doctor of Technical Sciences (1998), Candidate of Technical Sciences (1988), Professor, Head of Department of the Electromechatronics and Computerized Electromechanical Systems, National University "Lviv Polytechnic". Lviv, Ukraine
***Research field*:** Control Systems of Vehicle Electric Drive; Renewable Energy; Energy Storage Systems; Mathematical Modeling and Synthesis of Energy-Based Control Systems

Ігор Зенонович Щур – доктор технічних наук (1998), кандидат технічних наук (1988), професор, зав. каф. Електромехатроніки і комп'ютеризованих електромеханічних систем Національного університету «Львівська політехніка». Львів, Україна

Игорь Зенонович Щур – доктор технических наук (1998), кандидат технических наук (1988), профессор, зав. каф. Електромехатроники и компьютеризированных электромеханических систем Национального университета «Львовская политехника», Украина

Yurii Olegovych Biletskyi – Candidate of Technical Sciences (2015), Assistance Professor of the Department of Electromechatronics and Computerized Electromechanical Systems, National University "Lviv Polytechnic". Lviv, Ukraine
***Research field*:** Control theory; Energy-Based Approaches of Control System Synthesis; Renewable Energy Sources; Modeling of Electromechanical and Electrotechnical Systems

Юрій Олегович Білецький – кандидат технічних наук (2015), доцент кафедри Електромехатроніки та комп'ютеризованих електромеханічних систем Національного університету «Львівська політехніка». Львів, Україна

Юрий Олегович Билецкий – кандидат технических наук (2015), доцент кафедры Електромехатроники и компьютеризированных электромеханических систем Национального университета «Львовская политехника», Украина